PAPER

Check for updates

Numerical estimation of drug loading contents in amphiphilic nanogels

Ante Markovina,[†][a] Clara López-Iglesias, [iD] [†][ab] Ruiguang Cui[a] and Daniel Klinger [iD] *[a]

Amphiphilic nanogels (ANGs) are promising colloidal carriers to improve bioavailability of poorly water-soluble drugs. In contrast to conventional hydrophilic nanogels, ANGs contain additional hydrophobic domains in their network to load hydrophobic cargos. However, optimizing drug loading remains labour-intensive due to the lack of quantitative tools that accurately capture the complex ANG−drug interactions. To address this limitation and assess drug compatibility, we developed a quantitative framework based on Flory−Huggins interaction parameters (χ). Key to our approach is the empirical adjustment of the correction factor α to account for unequal contributions of dispersion forces, polar interactions, and hydrogen bonds. Using a model ANG and a library of hydrophobic drugs and dyes, we established selection rules for α based on the dominant interaction type: $\alpha = 1$ for dispersion-dominated, $\alpha = 0.7$ for polar, and $\alpha = 0.3$ for hydrogen bond-dominated systems. This enabled systematic grouping of cargos and revealed strong monotonic negative correlations between adjusted χ values and experimental loading capacities. The resulting universal calibration curve links χ to drug loading content across diverse ANG−drug systems. Consequently, our framework suggests predictive potential of solubility parameter-based models, reduces experimental burden, and supports the rational design of ANG carriers tailored to specific hydrophobic drugs.

1. Introduction

Formulation of poorly water-soluble drugs is a key challenge in pharmaceutical drug development.[1–3] To enhance solubility and increase bioavailability of hydrophobic drugs, polymer colloids have evolved as versatile delivery vehicles.[4–7] Among such nanocarriers, nanogels offer distinct advantages due to their crosslinked internal network. This provides high water content, mechanical flexibility, structural stability, and the ability to control loading and release profiles by stimuli-responsive swelling or degradation.[8–13] However, in conventional nanogels, the overall hydrophilic network limits efficient encapsulation of hydrophobic drug molecules.[10,14]

To overcome this limitation, amphiphilic nanogels (ANGs) contain random copolymer networks with both hydrophilic and hydrophobic side groups.[15] Within these hydrogel particles, the hydrophobic groups self-assemble into distinct domains that can encapsulate poorly water-soluble compounds.[16] Here, loading and release profiles depend on the polarity and number of the network's side groups.[17–19] While these features demonstrate the potential of ANGs as carriers for poorly water-soluble drugs, a detailed understanding of the underlying structure–property relations is lacking. Such insight is crucial to assess loading profiles for specific ANG–drug combinations and to guide the molecular design of customized carriers. To approach this, quantitative descriptors for cargo–network interactions and their correlation with experimental loading data are required.

Early efforts to address this need only considered the cargo's affinity to the hydrophobic domains.[20,21] In such approaches, the hydrophobic groups' partitioning coefficient (cLogP) was used as numerical descriptor to maximize drug–network interaction. However, this strategy neglects the influence of complex drug structures, which may also contribute to polar interactions. For example, recent spectroscopic studies on encapsulated Nile red suggest that hydrophilic interactions between cargo and hydrogel matrix play a significant role in loading as well.[22] Therefore, multiple contributions need to be considered when estimating molecular nanogel–cargo interactions.[23,24]

Hansen solubility parameters (HSPs) consider all these contributions through individual parameters (δ) that account for dispersion forces (δ_D), hydrogen bonds (δ_H), and polar

[a] *Freie Universität Berlin, Institute of Pharmacy, Königin-Luise Straße 2–4, 14195 Berlin, Germany*

[b] *Department of Pharmacology, Pharmacy and Pharmaceutical Technology, I + D Farma group (GI-1645), Faculty of Pharmacy, Instituto de Materiales (iMATUS) and Health Research Institute of Santiago de Compostela (IDIS), Universidade de Santiago de Compostela, Campus Vida s/n, 15782 Santiago de Compostela, Spain. E-mail: daniel.klinger@fu-berlin.de*

† Equal contribution.

2578 | *J. Mater. Chem. B*, 2026, **14**, 2578–2593

This journal is © The Royal Society of Chemistry 2026

Paper

forces (δ_P).[25,26] They can be obtained from molecular dynamics (MD) simulations, or through theoretical group contribution methods (GCM), *e.g.*, the Hoftyzer–van Krevlen (HVK)[27] or the Yamamoto molecular break (YMB)[28,29] method. However, they only provide qualitative correlations.[29] As an alternative, Flory–Huggins interaction parameters (χ) can be used to describe polymer–drug interactions.[27,30–32] These parameters can be determined experimentally[33,34] or also derived from the individual HSPs by considering molar volumes and a correction factor α. In a recent study, this approach was used to calculate χ for combinations of 18 different poly-2-oxazoline-based ABA triblock co-polymers with 4 drugs (paclitaxel, curcumin, efavirenz and thashinone IIA).[29] Unfortunately, for all drug–polymer pairs, a direct correlation between χ and experimental loading contents only showed limited quantitative accuracy. Thus, it was suggested that the more detailed partial solubility parameters should be considered to estimate drug–carrier interactions in this case.

In contrast to these limitations, we recently showed that GCM-derived Flory–Huggins parameters can indeed quantify interactions between ANGs and hydrophobic compounds. Key to successful quantification is the careful empirical adjustment of the correction factor α.[32] Conventionally, α is set to 1. According to Hansen, this simplified approach performs well for systems where dispersion forces dominate over polar and hydrogen-bonding ones.[25,35] However, it shows limitations in systems with strong polar interactions and hydrogen bonding.[36–39] Accounting for this non-ideal behavior, α can be reduced ($\alpha < 1$) to empirically correct for the shifted relative contributions of dispersion forces, polar interactions, and hydrogen bonding. This pragmatic approach enabled good quantitative description of the interaction between ANGs and oils of different polarity and structure.[40] Consequently, we suggest that similar considerations could enable quantitative description of drug–ANG interactions. For this, we aim to establish α as empirical correction factor that allows fine-tuning the balance between different interaction types in ANG–drug combinations. Focusing on the development of standardized selection rules for α, we aim to generalize this approach and improve the quantitative accuracy of Flory–Huggins parameters for systems involving hydrogen bonding.[32]

In systematically approaching this objective, we combine different ANGs with various hydrophobic drugs and dyes. In the present study, we focus on a well-defined class of amphiphilic nanogels based on poly(methacrylamide) copolymers, which serve as a model system to develop and validate the proposed framework under controlled and systematically varied conditions. To evaluate the influence of network hydrophobicity, we vary the structure of hydrophobic side groups and the ratio of hydrophilic and hydrophobic groups in the networks. To investigate the influence of cargo structure, we selected structurally diverse drugs and dyes to cover a broad range of functional groups. Having access to this library of drug–ANG combinations, we first analyze the interaction of a single type of nanogel with multiple drugs and dyes to establish a general strategy for fine-tuning the correction factor α in the calculation of χ. This adjustment is based on optimizing the correlation between calculated χ values and experimentally determined loading capacities (LC). Next, we examine the connection between χ and LC for selected model cargos in various nanogels. This allows us to assess the influence of structure and number of hydrophobic groups in the nanogel network. Ultimately, we construct a universal calibration curve by correlating Flory–Huggins interaction parameters and loading capacities across all tested nanogels and cargos. This enables the selection of hydrophobic groups to maximize loading content for a given drug, thus providing a rational framework to customize nanogels for specific drug delivery applications.

2. Results and discussion

Loading hydrophobic compounds in amphiphilic nanogels depends on multiple interactions between cargo, hydrophobic domain, and the surrounding network (see Scheme 1a). The
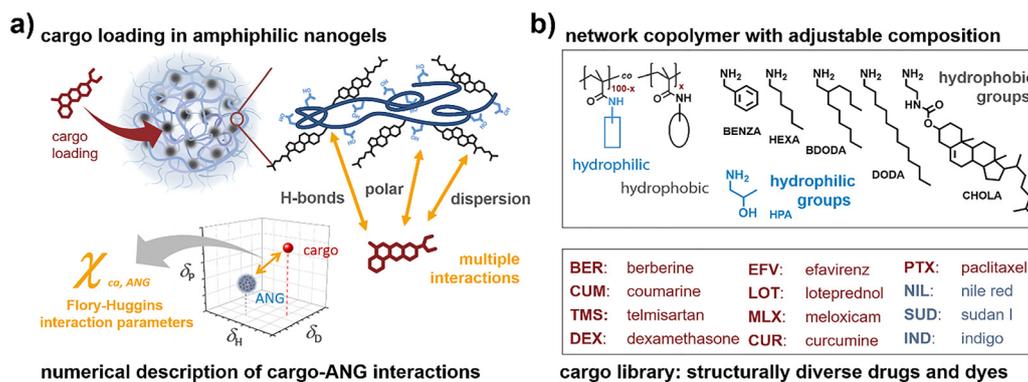
Scheme 1 Cargo loading in amphiphilic nanogels (ANGs) depends on multiple interactions that vary with ANG network composition and cargo structure. (a) Flory–Huggins interaction parameters can be derived from 3D Hansen solubility parameters and provide numerical descriptors for cargo–ANG interactions. (b) The influence of ANG network composition and cargo structure can be determined by combining a library of ANGs with multiple drugs and dyes. In the ANG library, the network hydrophobicity can be controlled through type and amount of hydrophobic side groups in random copolymers.

relative contribution of dispersion forces, polar forces, and hydrogen bonding is determined by the structure of the drug and the molecular composition of the network copolymer, *i.e.*, the ratio between hydrophilic and hydrophobic side groups and their respective structures. Thus, to examine the influence of the nanogel structure, we designed a library of amphiphilic nanogels with varying network composition (see Scheme 1b). The ANGs are based on poly(methacrylamide) copolymers that combine hydrophilic 2-hydroxypropylamide (HPA) side groups with varying ratios of different hydrophobic side groups, *i.e.*, benzylamide (BENZA), hexylamide (HEXA), dodecylamide (DODA), branched dodecylamide (BDODA), and cholesterylamide (CHOLA).[20] This library was then used to determine the loading content with a selection of hydrophobic drugs (dexamethasone, coumarin, meloxicam, paclitaxel, curcumin, loteprednol and telmisartan) and dyes (indigo, berberine, Nile red and Sudan I) (Scheme 1b). These cargos were selected to cover a broad variety of structural elements, *e.g.*, aromatic rings, fluorine groups, anionic groups, cationic groups, H-donors, H-acceptors, and steroid frameworks. With these libraries, we aim to span a wide range of possible drug–nanogel interactions that are required to determine the potential of ANGs for therapeutic delivery applications. Accordingly, the present study does not aim to cover chemically distinct nanogel systems, but instead uses this well-defined platform as a model system to develop and test the proposed correlation framework.

2.1. Developing a library of amphiphilic nanogels with hydrophobic cargos

Synthesis of nanogels with varying network hydrophobicity. To accurately assess how molecular network composition affects loading in ANGs, we needed comparable particles: the ANGs in the library should vary only in their chemical composition while maintaining similar colloidal features such as crosslinking density, crosslinker distribution, size, and size distribution. This can be provided by functionalizing a master batch of crosslinked reactive precursor particles with different mixtures of hydrophilic and hydrophobic groups.[20,41] By decoupling network functionalization from particle synthesis, all particles show similar colloidal properties that are governed by the precursors. As a result, comparability is ensured.[41]

This strategy uses emulsion polymerization for the preparation of precursor particles from crosslinked poly(pentafluorophenyl methacrylate) (PPFPMA). In PPFPMA, the reactive ester side groups enable network functionalization with mixtures of hydrophilic 2-hydroxypropylamine (HPA) and various hydrophobic amines to give a library of amphiphilic nanogels with a P(HPA-*co*-hydrophobic) network (see Scheme 1 and SI, Fig. S1).[40] This library consists of two particle sets (Scheme 2): in set 1, the structure of the hydrophobic group was varied while keeping the molar ratio between hydrophilic and hydrophobic groups on the polymer network constant. This set of amphiphilic nanogels contains always 80 mol% of HPA and 20 mol% of different hydrophobic groups, *i.e.*, hexylamine (HEXA), benzylamine (BENZA), linear dodecylamine (DODA), branched dodecylamine (BDODA), and an amine-functionalized cholesterol
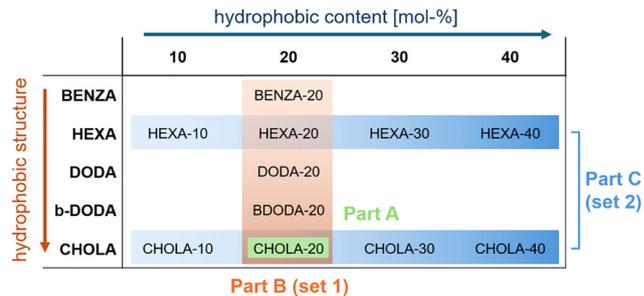
Scheme 2 The library of amphiphilic nanogels with different network compositions consists of two different particle sets: in set 1, the structure of the hydrophobic group is varied while the molar ratio between hydrophilic and hydrophobic groups is held constant. This set of ANGs always contains 80 mol% of HPA and 20 mol% of different hydrophobic groups, *i.e.*, hexylamine (HEXA), benzylamine (BENZA), linear dodecylamine (DODA), branched dodecylamine (BDODA), and an amine-functionalized cholesterol (CHOLA). In set 2, the content of hydrophobic groups is varied from 10 to 40 mol% for two fixed hydrophobic structures, *i.e.*, HEXA and CHOLA. These two hydrophobic groups were chosen as representatives for high and medium hydrophobicity, respectively.

(CHOLA). Particles are denoted respectively: BENZA-20, HEXA-20, DODA-20, BDODA-20, CHOLA-20 (see SI, Fig. S2 for characterization). This set includes CHOLA20 as an established model ANG with a fixed amount of one specific hydrophobic group. In set 2, the content of hydrophobic groups was varied from 10 to 40 mol% for CHOLA and HEXA-based ANGs. These two hydrophobic groups were chosen as representatives for high and medium hydrophobicity, respectively. Changing the hydrophilic/hydrophobic ratio led to two groups of ANGs with precisely tuned amphiphilicity, *i.e.*, CHOLA-10 to CHOLA-40 and HEXA-10 to HEXA-40 (see SI, Fig. S3 for characterization).

After network functionalization, the nanogels were successfully transferred to water and angle-dependent dynamic light scattering (DLS) showed hydrodynamic diameters around 160 nm with narrow size distributions, independent of network composition (see SI, Fig. S5). The particle size remained stable over weeks, indicating good long-term colloidal stability. Transmission electron microscopy (TEM) revealed homogeneous particle morphologies with no distinct microphase separation (see SI, Fig. S4). Overall, this approach allowed preparing a library of ANGs with similar colloidal features and network copolymers that combine the biocompatible hydrophilic features of poly(*N*-(2-hydroxypropyl) methacrylamide) (PHPMA) with the hydrophobic nature of aliphatic and aromatic amines (see SI, Fig. S6).

Loading of amphiphilic nanogels with hydrophobic cargos. Developing quantitative tools for ANG–drug loading requires experimental loading data that can be correlated with numerical descriptors for cargo–network interactions. Thus, experimental loading contents (LC) were determined as mass ratio of drug to ANG. This was attempted on CHOLA-20 particles as model system *via* two different methods: the co-solvent and the film uptake method (Experimental section for details).

In each method, CHOLA-20 nanogels were combined with a feed ratio of 10 wt% (w.r.t. ANG) of different hydrophobic drugs
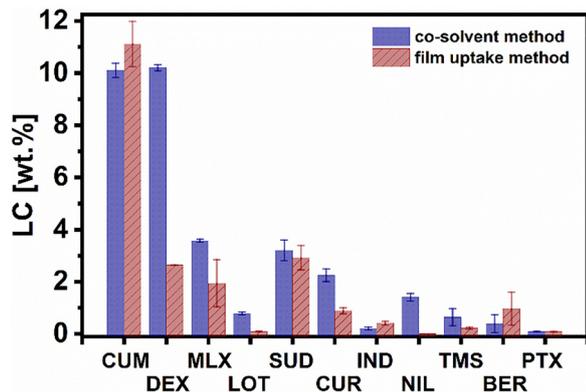
2580 | *J. Mater. Chem. B*, 2026, **14**, 2578–2593

This journal is © The Royal Society of Chemistry 2026

Fig. 1 CHOLA-20 particles serve as model ANGs to evaluate the influence of loading procedure for the cargo library. In comparison, the average loading contents (LCs) from the co-solvent method are higher than the LCs from the film uptake method.

and dyes. Investigated drugs were: dexamethasone, coumarin, meloxicam, paclitaxel, curcumin, loteprednol, and telmisartan. Examined dyes were: indigo, berberine, Nile red, and Sudan I. After the loading procedure, LCs were determined *via* UV/Vis spectroscopy or *via* reverse phase-HPLC and the results of both loading methods are compared in Fig. 1 (see SI, Fig. S7–S17 for calibration curves). On average, the co-solvent method results in higher LCs than the film uptake method. Especially dexamethasone (DEX), meloxicam (MLX), curcumin (CUR), and Nile red (NIL) showed higher loading. As control, the results for Nile red are consistent with our previous work.[20] Based on the higher LCs, the co-solvent method was selected as standard loading protocol for all further experiments.

2.2. Calculating solubility parameters for amphiphilic nanogels and cargos

Hansen solubility parameters for amphiphilic nanogels. To correlate the experimental LCs to quantitative cargo–network interactions, numerical descriptors are required that capture essential chemical and structural characteristics of the network and the cargo. For this, we used Flory–Huggins interaction parameters between drugs/dyes and nanogels. Their calculation is based on the respective Hansen solubility parameters (δ). For the ANGs, HSPs were calculated for the network forming copolymers.[25] In this approach, the individual contributions from dispersion forces (F_D), polar forces (F_P), and the energy of hydrogen bonds (E_H) are considered as partial solubility parameters δ_D, δ_P, and δ_H respectively. Each parameter can be assessed by indirect group contribution methods (GCM), which divide the attractive forces and hydrogen bonding energy of a molecule into structural group contributions $F_{D,i}$, $F_{P,i}$, and $E_{H,i}$. These contributions are then summed and translated into the partial solubility parameters by adjusting with the molar volume (V_m) of the molecule (see experimental part). We employed two different methods to calculate these forces and energies for the network copolymers:

First, we used the Hoftyzer–van Krevlen method (HVK), which relies on tabulated values for the individual structural

group contributions.[27] To account for the changing composition in the P(HPA-*co*-hydrophobic) network copolymers, we considered the molar fractions of the different monomers, *i.e.*, f_{HPA} and $f_{hydrophobic}$. With this, the total force or energy of a given copolymer was calculated as the weighted sum of its monomeric components, *e.g.*, $F_D = f_{HPA} \cdot F_{D,PHA} + f_{hydrophobic} \cdot F_{D,hydrophobic}$ (see Experimental section for details). A similar weighted approach was used to determine molar volumes *via* Fedors' method, which is also based on tabulated group contribution values (see SI, Section 2.1).[42]

Second, we used the Yamamoto molecular break (YMB) method to calculate the HSPs of the ANGs' networks. This method is integrated into the commercially available software Hansen solubility parameters in practice (HSPiP), where partial solubility parameters can be directly assessed from the SMILES codes of each chemical compound (obtained from ChemDraw Professional 15.2.). To account for the changing copolymer composition in the P(HPA-*co*-hydrophobic) network copolymers, we used the "polymer blends" option,[25] which considers the copolymer as a blend of two homopolymers, *i.e.*, P(HPA) + P(hydrophobic). The molar ratio between HPA groups and hydrophobic groups is considered through the corresponding weight fraction of each homopolymer. To determine the molar volumes of the copolymers, we used our weighted Fedors' group contribution method (see SI, Tables S1–S7). Similarly, for the drugs, the same approach was made to determine the molar volumes (see SI, Tables S8–S19, Fig. S18).

Solubility parameters for the ANGs from both methods are compared in Fig. 2 (also see SI, Table S7). This data reveals three general trends: (1) effect of calculation methods. Both GCMs (YMB and HVK) show similar trends in how solubility parameters change with nanogel composition. However, YMB generally yields higher values than HVK. (2) Effect of hydrophobic groups. For nanogels containing a specific hydrophobic group, solubility parameters decrease as the molar content of that group increases. For example, in CHOLA-functionalized nanogels, the polar solubility parameter δ_P (YMB) decreases from 15 to 10 MPa$^{1/2}$ as the CHOLA-content increases from 10 to 40 mol% (see Fig. 2a). Interestingly, the dispersion parameter δ_D from YMB calculations deviates from this trend, as δ_D (YMB) remains largely unaffected by the content of hydrophobic groups (Fig. 2b). Another deviation is observed for δ_D of BENZA-functionalized nanogels. Here, δ_D increases with BENZA-content, highlighting the unique influence of aromatic groups on dispersion forces (Fig. 2b). (3) Effect of carbon chain length. For nanogels with a fixed hydrophobic group content, solubility parameters decrease upon increasing the carbon number in these hydrophobic side groups. For example, in nanogels with 40 mol% hydrophobic groups, the hydrogen bonding parameter δ_H (YMB) gradually decreases from 12 to 8 MPa$^{1/2}$ as hydrophobic groups change from BENZA to CHOLA in the following order: BENZA-40 > HEXA-40 > BDODA-40 > DODA-40 > CHOLA-40 (Fig. 2c).

Overall, these trends translate to the total solubility parameters δ_T (YMB) and δ_T (HVK), where deviations in dispersion parameters are balanced by other contributions (Fig. 2d). As a

This journal is © The Royal Society of Chemistry 2026

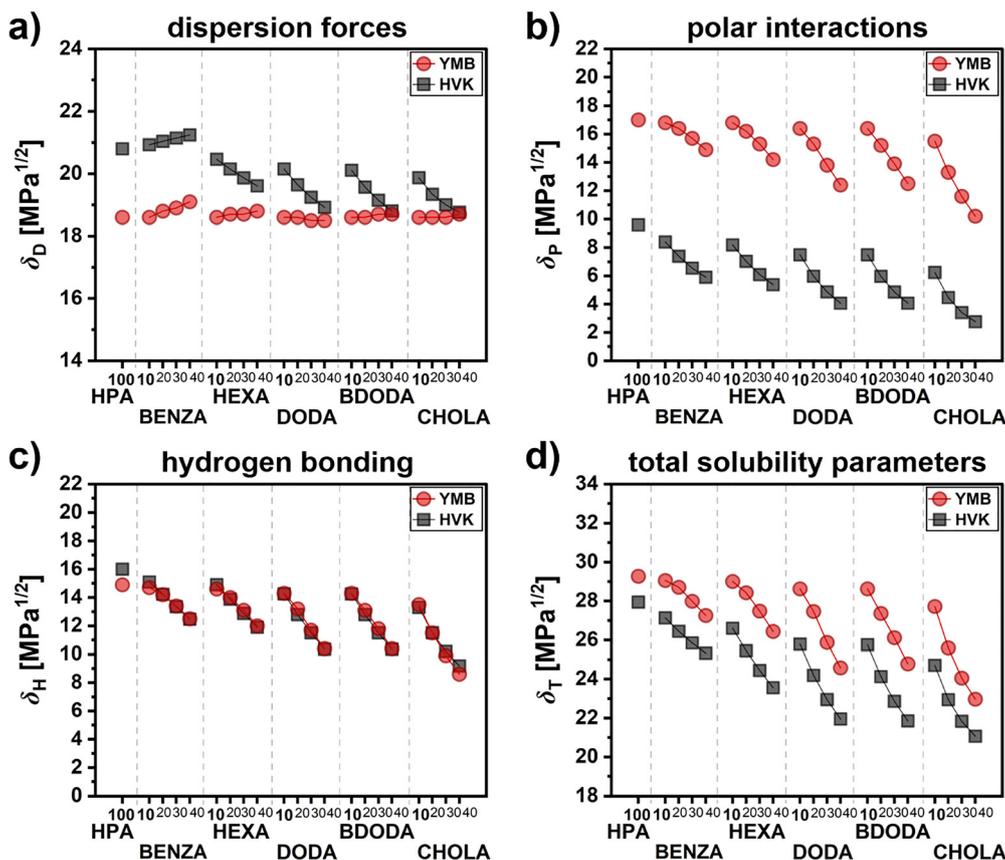*J. Mater. Chem. B*, 2026, **14**, 2578–2593 | **2581**

Fig. 2 Hansen solubility parameters decrease with the number of hydrophobic groups in ANGs with a fixed structure of hydrophobic groups. This behavior is observed for the individual solubility parameters that represent the contributions of (a) dispersion forces, (b) polar interactions, and (c) hydrogen bonding to the total solubility parameter (d). The trend is observed for data from both the HVK and the YMB methods.

result, the total solubility parameter can be used to compare network hydrophobicity between nanogels. For example, the similar δ_T (YMB) values for BENZA-40, HEXA-30, DODA-20, BDODA-20 and CHOLA-10 nanogels suggest that these samples share comparable network hydrophobicity.

Hansen solubility parameters for drugs and dyes. For the cargos, solubility parameters were calculated by the same group contribution methods as for the ANGs, i.e., HVK and YMB. When comparing the calculated solubility parameters across the cargo library, only a few drugs showed similar values for both methods (see SI Fig. S18). For the dispersion component (δ_D), SUD and TMS exhibited similar values, while for the polar component (δ_P), only BER showed good agreement between HVK and YMB. Greater consistency was observed for the hydrogen bonding component (δ_H) and the total solubility values (δ_T): COU, MLX, and BER had similar δ_H values, while COU, MLX, CUR, and NIL showed similarities in δ_T. The differences between δ (YMB) and δ (HVK) for some drugs and dyes may be due to missing experimental values for the forces and energies of specific structural groups in the HVK method, e.g., molar attractive forces (F_{di}, F_{pi}) and energy of hydrogen bonding (E_{hi}).[27] In those cases, the most chemically similar functional groups were used for the calculations (see SI Tables S9–S19).

2.3. Correlating Flory–Huggins parameters to drug loading capacities

The Hansen solubility parameters form the basis for the calculation of Flory–Huggins interaction parameters (χ). Correlating these numerical descriptors for cargo–network interactions with experimental loading capacities proceeds in four key stages (Scheme 2): (1) part A: we develop standardized criteria for adjusting the empirical correction factor α to different cargo structures. These criteria are designed to account for the shifted balance between hydrogen bonding and dispersion/polar interactions when calculating χ for ANG–cargo combinations. To highlight the influence of cargo structure, we focus on CHOLA-20 as model ANG system and combine it with our entire cargo library. (2) Part B: we apply the developed α-selection criteria to the calculation of interactions between cargos and ANGs of varying network hydrophobicity, i.e., different structure of hydrophobic groups but similar ratio to hydrophilic groups. Using three representative cargos, we assess whether our approach enables reliable correlations between calculated interaction parameters and experimentally determined loading capacities. (3) Part C: we extend the evaluation by testing ANGs with different molar ratios of hydrophobic groups. Specifically, we examine nanogels functionalized with HEXA (low hydrophobicity) and CHOLA (high hydrophobicity) to determine how

2582 | J. Mater. Chem. B, 2026, **14**, 2578–2593

This journal is © The Royal Society of Chemistry 2026

well the adjustment of α performs across a broader range of network compositions. (4) Integration: finally, we integrate all results to assess whether the α-adjusted interaction parameters reliably correlate with experimental loading capacities across diverse ANG–cargo combinations. A successful correlation would offer a practical guideline for optimizing ANG composition to maximize drug loading for any given cargo.

Part A: correlating Flory–Huggins interaction parameters with experimental drug loading capacities by developing standardized selection criteria for α

Calculation of Flory–Huggins interaction parameters ($\chi_{ca,ANG}$) uses the individual Hansen solubility parameters for ANG ($\delta_{D,ANG}$, $\delta_{P,ANG}$, $\delta_{H,ANG}$) and cargo (ca) ($\delta_{D,ca}$, $\delta_{P,ca}$, $\delta_{H,ca}$) as shown in eqn (1). Here, directional constraints of hydrogen-bonds and bond-like dipole–dipole interactions are considered by introducing the factor 0.25 for their solubility terms.[25] Typically, this modified equation accounts for different mixing behaviours in polymer–solvent systems through the correction factor α.[35]

$$\chi_{ca,ANG} = \alpha \frac{V_{m,ca}}{RT}\Big(\big(\delta_{D,ca} - \delta_{D,ANG}\big)^2 + 0.25\big(\delta_{P,ca} - \delta_{P,ANG}\big)^2 + 0.25\big(\delta_{H,ca} - \delta_{H,ANG}\big)^2\Big) \quad (1)$$

Hansen suggested the use of $\alpha = 1$ for systems where dispersion forces dominate.[25,35] However, this simplified correction has limitations in systems with strong contributions from polar forces and hydrogen bonding.[32,37,38] Here, more adequate representations of χ can be obtained by empirically reducing α ($\alpha < 1$).[35,43,44] Nevertheless, transferring such empirical adjustments to a reliable quantification of drug–ANG interactions ($\chi_{ca,ANG}$) requires standardized selection rules for α that take into account the structural diversity of cargo molecules.

In developing such selection rules for our ANGs, we focused on one model nanogel (CHOLA-20) and tested it with different cargos. Reducing the ANG library to a single sample provides a consistent ANG matrix to isolate the cargos' structural influence on cargo–ANG interactions. In this framework, the cargos act as the variable factor, similar to solutes in classical solubility parameter theory. Here, individual molecules are characterized by their dispersive, polar, and hydrogen-bonding contributions. Thus, differences in cargo–ANG interactions are attributed directly to the inherent physicochemical properties of the cargos as follows: for strongly hydrophobic cargos, we suggest that dispersion forces dominate the cargo's interactions with the hydrophobic nanodomains in the ANGs. For cargos with increasing polarity, we assume that additional interactions with the ANGs' hydrophilic regions appear, *i.e.*, dipolar interactions and hydrogen bonding.[22] As a result, each cargo–ANG combination is represented by a specific balance of these three different interaction forces. We suggest that an accurate description of the cargo–ANG interactions requires a theoretical framework that takes this balance into account. For this, we identified three distinct selection criteria to distinguish the relative

contributions of the individual Hansen solubility parameters. These criteria were used to divide the cargo library into three different groups based on whether ANG–cargo interactions are primarily governed by:

(1) Dispersion forces: $\alpha = 1$ for $\delta_D > (\delta_P + \delta_H)$

Selection criterium: dispersion forces are stronger than combined polar and hydrogen bonding interactions.

(2) Polar interactions: $\alpha = x$ for $\delta_D < (\delta_P + \delta_H)$, but $\delta_P > \delta_H$

Selection criterium: combined polar and hydrogen bonding forces are stronger than dispersion forces. Additionally, polar interactions are stronger than hydrogen bonding interactions.

(3) Hydrogen bonding: $\alpha = y$ for $\delta_D < (\delta_P + \delta_H)$, but $\delta_H \geq \delta_P$

Selection criterium: combined polar and hydrogen bonding forces are stronger than dispersion forces. But, hydrogen bonding interactions are stronger or equal than polar interactions.

These selection rules were applied to sort all drugs and dyes from our library into groups to optimize the α values (Fig. 3). Overall, different groups are obtained whether individual solubility parameters were derived using the HVK or the YMB method. In group 1, dispersion forces dominate for COU, CUR, TMS, BER and NIL from the HVK method, and for PTX, TMS, BER, NIL and SUD from the YMB method. Group 2 reflects an increasing influence of polar interactions. This group only contains COU, MLX and SUD for the YMB method. Group 3 reflects the additional influence of hydrogen bonds. This was observed for DEX, MLX, PTX, LOT and SUD (HVK method), and for DEX, CUR and LOT (YMB method). Interestingly, both methods only assigned TMS, BER, NIL, DEX and LOT to the same group.

After defining standardized criteria to distinguish cargo–ANG interactions, we focused on optimizing specific α values to calculate Flory–Huggins interaction parameters between each cargo and our model ANG (CHOLA-20). We hypothesize that such corrected values for $\chi_{ca,ANG}$ enable quantitative correlations with the experimentally determined loading contents. To evaluate this hypothesis, we assign an empirical value for α to correct the relative influence of dispersion forces. For group 1 (dispersion-dominated), we follow Hansen's original approach and use $\alpha = 1$.[25] For group 2 (polar-dominated) and group 3 (H-bond-dominated), α is variable and requires empirical optimization, *i.e.* we set $\alpha = x$ for group 2 and $\alpha = y$ for group 3. This grouping method to distinguish dominant interaction types is in direct contrast to established approaches where a constant α value is used independent of the cargos structure. On one hand, Hansen used $\alpha = 1$ for various solvents (cargos) and showed that this approximation is only accurate for systems with dominant dispersion forces. On the other hand, a method proposed by Lindvig accounts for both polar and hydrogen-bonding contributions but applies a single, uniform α value of 0.6 to all interactions.[35] As a result, these established approaches cannot reflect the cargo-specific balance between polar and hydrogen-bonding interactions.

In our approach, we started α optimization with values that reflect both theoretical principles and empirical observation (see SI, Table S22). For cargos in which dispersion interactions
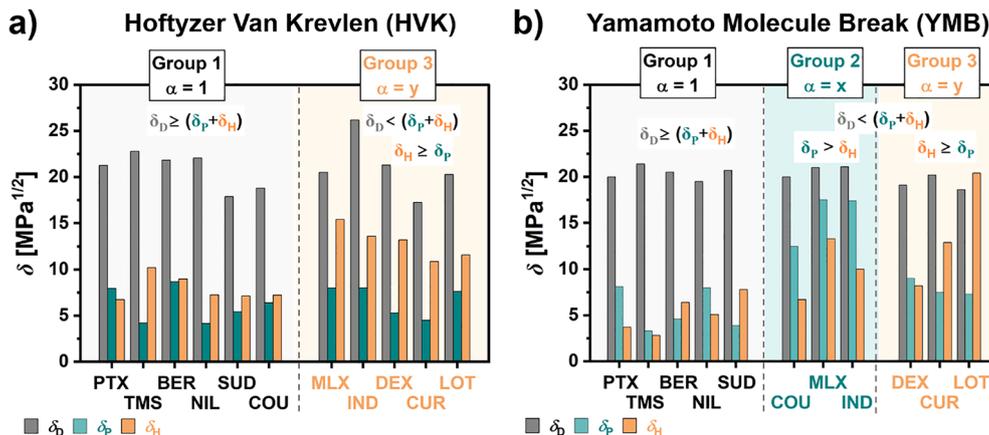
This journal is © The Royal Society of Chemistry 2026

J. Mater. Chem. B, 2026, **14**, 2578–2593 | **2583**

Fig. 3 The correction factor α serves as numerical descriptor for the relative contributions of dispersion forces (δ_D), polar interactions (δ_P), and hydrogen bonds (δ_H) in each cargo molecule. Three groups can be distinguished that are assigned different values for α: group 1 (α = 1): dispersion forces are stronger than combined polar and hydrogen bonding interactions. Group 2 (α = x): combined polar and hydrogen bonding forces are stronger than dispersion forces. Additionally, polar interactions are stronger than hydrogen bonding interactions. Group 3 (α = y): combined polar and hydrogen bonding forces are stronger than dispersion forces, but hydrogen bonding interactions are stronger or equal than polar interactions. Application of these selection rules results in distinct groups of cargo molecules depending on the method that is used for the calculation of the underlying solubility parameters, *i.e.*, the HVK method (a) or the YMB method (b).

are dominant (group 1), α = 1 was used. In accordance with Hansen's original framework, this provides a reference standard for predominantly hydrophobic molecules. For polar- and H-bond-dominated cargos (groups 2 and group 3), we used intermediate values that were previously derived from ANG–solvent systems with known predominant forces: α = 0.6 has been shown to accurately capture polar interactions in ANG–solvent systems and was therefore applied for cargos of group 2. In addition, α = 0.3 was empirically determined to account best for the dominating H-bonds in ANG–water combinations and therefore used for cargos of group 3.[40]

The accuracy of the selected α values was evaluated by examining the correlation between calculated χ and experimentally determined LC. Corrected Spearman's correlation coefficients (ρ) were used as quantitative non-parametric measures of the correlation (see SI, Table S22). The results were compared to previously established approaches, namely Lindvig's method (α = 0.6 for all cargos) and Hansen's original framework (α = 1 for all cargos). For calculated data from the HVK method, no significant correlation was observed (ρ < −0.3). In contrast, for the YMB method, our approach yielded ρ = −0.87, compared to ρ = −0.85 for Lindvig's method, and ρ = −0.83 for Hansen's framework. These non-optimized results indicate reasonable agreement with the literature and represent a good starting point for further optimization. We assume that the explicit differentiation between polar- and hydrogen-bond-dominated cargos could further improve model performance upon empirical variation of α.

To explore this systematically, we evaluated ρ across a matrix of α values individually assigned to each cargo group: α was varied from 0.1 to 1 for polar-dominated cargos and similarly from 0.1 to 1.0 for hydrogen-bond-dominated cargos. In contrast, dispersion-dominated cargos were held constant at α = 1. Corrected Spearman correlation coefficients for all combinations

are presented in the SI Fig. S19. For the HVK method, poor correlation was observed across all examined α values (see SI, Fig. S19a). We assume that the poor correlation may be due to inaccurate calculations of the underlying solubility parameters of selected cargos. Although the HVK method performed particularly good in ANG–solvent systems, where tabularized data is accessible,[40] correct values for the molar attractive forces (F_{di}, F_{pi}) and hydrogen bonding energies (E_{hi}) are not available for some functional groups of the cargos (see SI, red values in Tables S10, S13, S14, S16 and S18). As a result, this can lead to incorrect estimates of $\chi_{ca,ANG}$ that simply cannot be corrected by α. For the YMB method, the initial screening indicated best correlation coefficients (ρ) for multiple combinations of α values from polar and hydrogen-bonding interactions (SI, Fig. S19b). These results do not point to a single optimal α parameter set, as several combinations of comparable performance were observed (marked in bright and dark green). To address this limitation, and to account for experimental variability in the determination of loading contents (LC ± SD), we extended our screening by applying a mathematical fit to describe the relationship between LC and χ. Specifically, an allometric power fit was used, as this model can capture strong, non-linear deviations between χ and LC that arise from the structural diversity and chemical complexity of the cargo. In allometric models, the relationship is typically expressed as LC = $a \times \chi^b$, where $b \neq 1$ reflects deviations from simple linear proportionality. The quality of the fits was evaluated using the corrected coefficient of determination (corr. R^2), providing a quantitative indicator of strong correlation. The corresponding values are shown in Fig. 4 and in the SI, Fig. S20.

Results from the HVK method did not show clear trends between α-adjusted $\chi_{ca,ANG}$ and LC for any of the examined α values assigned to hydrogen-bonding interactions. All correlation coefficients from allometric fits are below 0.15 (see SI, Fig. S20). Even after using α = 0.1 (Fig. 5a), which gives the best

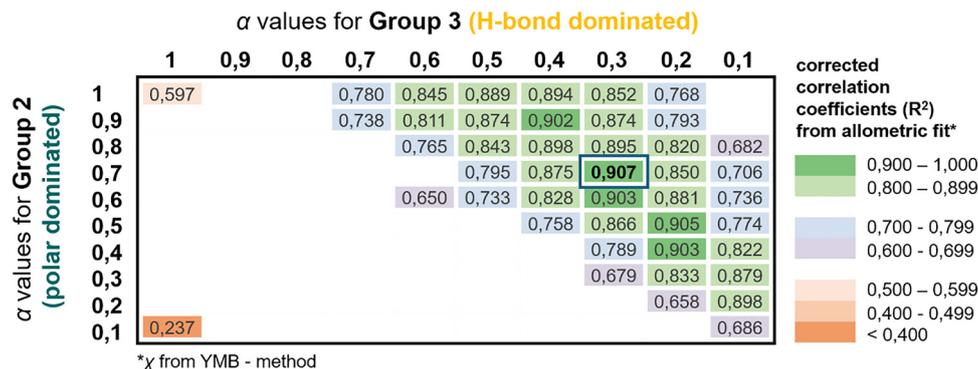Fig. 4 Optimization of α values for cargos of group 2 and group 3 by analysing the correlation between experimental LC and α-adjusted χ (from YMB). Corrected correlation coefficients (R^2) of allometric fits between LC and χ serve as quantitative measure for correlation and suggest optimum values of $\alpha = 0.7$ for group 2 and $\alpha = 0.3$ for group 3 ($R^2 = 0.907$).
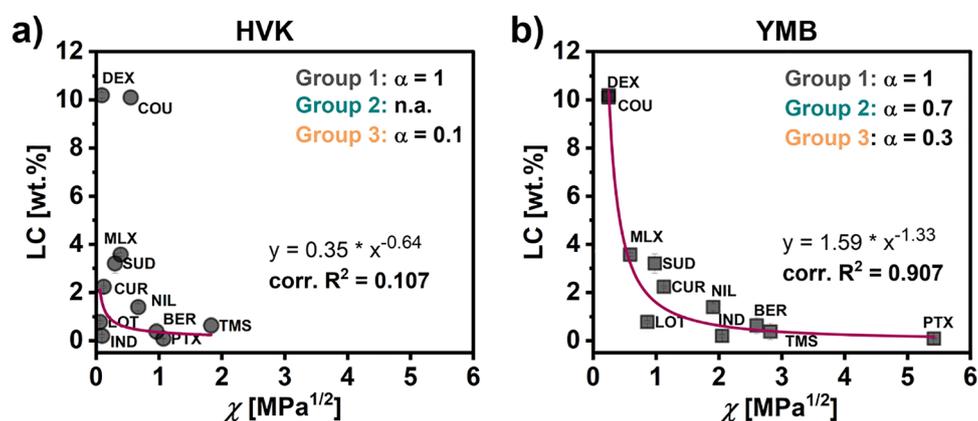

Fig. 5 Combination of cargo library with CHOLA-20 ANGs – correlation of experimental loading contents (LC) with α-adjusted Flory–Huggins interaction parameters ($\chi_{ca,ANG}$). For optimized α values, the quality of allometric fit depends on the calculation method for the underlying Hansen solubility parameters: (a) for the HVK method, LC does not correlate well with $\chi_{ca,ANG}$ ($R^2 = 0.107$). (b) For the YMB method, a clear negative monotonic relationship between $\chi_{ca,ANG}$ and LC is observed that can be fitted with a power function (corrected correlation coefficient: $R^2 = 0.907$).

correlation coefficient of $R^2 = 0.107$, the correlation did not improve compared to results from non-adjusted values, *i.e.*, using $\alpha = 1$ for all cargos ($R^2 = 0.112$, but $b > 0$ in allometric fit) (see SI, Fig. S21). Thus, suggesting that this method is not suited for accurately capturing cargo–ANG interactions.

For data from the YMB method (Fig. 4), corrected coefficients of determination (R^2) are substantially higher than for the HVK method (SI, Fig. S20). Here, an optimum value of $R^2 = 0.907$ suggests good correlation for optimized α values of 0.7 and 0.3 for polar and hydrogen-bonding interactions, respectively. These α values are close to our previous model and their application outperforms Lindvig's model, where a uniform $\alpha = 0.6$ is applied to both polar interactions and hydrogen bonds ($R^2 = 0.650$), and surpasses Hansen's original framework, where $\alpha = 1$ is used for all cargos ($R^2 = 0.597$) (Fig. 4 and SI, Fig. S21). Using these optimized α values results in an allometric fit with a clear trend between α-adjusted $\chi_{ca,ANG}$ and LC: LC increases as the χ decreases (Fig. 5b). This supports our hypothesis and highlights the importance of systematically accounting for the different interactions in the

calculation of χ. Importantly, a steep increase in LC is observed for $\chi_{ca,ANG} < 0.5$, which is commonly considered as a threshold for two components to be completely miscible.[45] Thus, the observed trend is in good agreement with the general Flory–Huggins theory. In addition, the two cargos with the highest LC (DEX and COU) were assigned α values of 0.3, indicating a considerable contribution of hydrogen bonds to the interaction with the ANGs. These findings suggest that high loading contents in amphiphilic nanogels are driven not only by dispersion forces between cargo and hydrophobic domains but also by polar interactions and hydrogen bonding with the hydrophilic PHPMA matrix.

Overall, our results indicate that combining individual solubility parameters from the YMB method with standardized selection criteria for α enables the calculation of $\chi_{ca,ANG}$ values that capture the complex interactions between cargos and ANGs. These quantitative values show a strong correlation with experimentally determined loading contents, thus suggesting a quantitative, correlation-based framework that has the potential to be developed into a predictive model. This potential

This journal is © The Royal Society of Chemistry 2026

J. Mater. Chem. B, 2026, **14**, 2578–2593 | **2585**

clearly surpasses that of conventional methods that use other numerical descriptors for cargo–ANG interactions. For example, Hildebrand solubility parameters (see SI, Fig. S22) or the Hansen distance (R_a) between drug and carrier in the 3-dimensional HSP space (see SI, Fig. S23, S25 and S27) provide only non-quantitative insights into cargo–ANG compatibility. As a result, no clear correlations with LC are observed.

Part B: influence of ANG hydrophobicity on correlation between LC and $\chi_{ca,ANG}$: variation of hydrophobic groups but similar hydrophobic/hydrophilic ratio

Development of tailored nanogel-based drug delivery systems would benefit from a numerical model that allows a researcher to answer the following question: "Which nanogel composition can maximize the loading content of this given drug?" Such an ability to identify the optimum nanogel structure could save tedious experimental tests and guide the carrier development early on.

In addressing this question, we first examined whether our previously developed model could guide the selection of hydrophobic structures in the nanogel network. For this, we examined whether experimental LCs correlate with calculated $\chi_{ca,ANG}$ values for ANGs with different hydrophobic groups. To isolate the structural influence of the hydrophobic groups, all networks contained a similar molar ratio between hydrophobic and hydrophilic groups, i.e., 20 mol% hydrophobic groups in BENZA-20, HEXA-20, DODA-20, BDODA-20, and CHOLA-20 (see set 1 in Scheme 2). These ANGs were each combined with three model cargos that show high (COU), medium (CUR), and low (NIL) LCs in the CHOLA-20 model ANGs. For each cargo, we calculated $\chi_{ca,ANG}$ using the YMB method and our developed selection criteria for α (see SI, Tables S25–S27). These values were then correlated with the respective experimentally determined LC.

As shown in Fig. 6, LCs increase with decreasing $\chi_{ca,ANG}$ (YMB) for each cargo. The negative monotonic relations are in good agreement with the classical Flory–Huggins theory where lower χ values indicate better miscibility, i.e., higher LCs. For all cargos, the relations are strongly linear with corrected R^2 values of 0.948 (COU), 0.946 (CUR), and 0.932 (NIL). We assume that

the linear correlations represent the systematic variation in ANG network composition that is also reflected in a systematic difference of the underlying solubility parameters (see Fig. 2). This contrasts the complex influence of cargo structure, where solubility parameters vary individually, reflecting structural diversity (see SI, Fig. S18). Overall, the high coefficients of determination suggest that loading of these cargos can be approximated as mixing cargos and network polymers, as indicated by $\chi_{ca,ANG}$. As a result, estimates from the YMB method could guide the selection of hydrophobic groups in ANGs to maximize LC for a given cargo (see SI, Fig. S24 for results from HVK method).

Part C: influence of ANG hydrophobicity on correlation between LC and $\chi_{ca,ANG}$: variation of hydrophobic/hydrophilic ratio for similar hydrophobic groups

We further investigated the influence of ANG hydrophobicity by varying the molar ratio between hydrophobic and hydrophilic groups in the nanogels' network. This was performed on two sets of ANGs that each contain a specific hydrophobic structure in combination with HPA as hydrophilic units (see Scheme 2). Set 2a consists of nanogels with 10–40 mol% of hydrophobic cholesteryl groups (CHOLA), i.e., CHOLA-10, CHOLA-20, CHOLA-30, and CHOLA-40. Set 2b contains ANGs with similar contents of hexyl groups (HEXA), i.e., HEXA-10, HEXA-20, HEXA-30, and HEXA-40. All ANGs were combined with our model cargos COU, CUR and NIL. For each ANG–cargo combination, $\chi_{ca,ANG}$ was calculated via the YMB method with adjusted α values (see SI, Tables S28–S30). The results were then correlated with the respective experimental LCs in Fig. 7.

For each individual cargo, LC increases monotonically with decreasing $\chi_{ca,ANG}$, thus agreeing with the general Flory–Huggins theory. Linear fits of the data showed strong correlations between $\chi_{ca,ANG}$ and LC values, i.e., corrected R^2 values of 0.923 for COU, 0.992 for CUR, and 0.940 for NIL. For all cargos, LC correlated equally well with both the molar ratio of hydrophobic groups and the type of hydrophobic groups (e.g., corr. R^2 = 0.992 (CUR) in Fig. 7b compared to corr. R^2 = 0.946 (CUR) in Fig. 6b). In contrast, calculating $\chi_{ca,ANG}$ via the HVK method did not show good correlations (SI, Fig. S26).
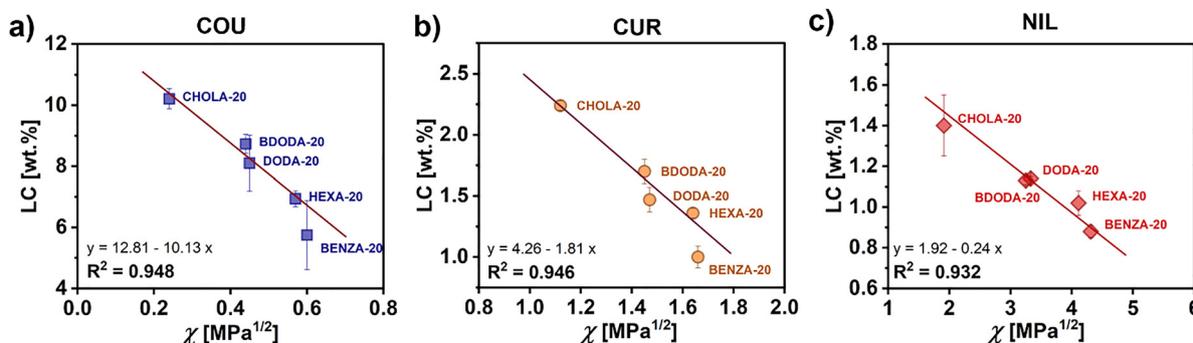

Fig. 6 Combination of COU, CUR, and NIL with ANGs containing 20 mol% of different hydrophobic structures – strong linear correlations are observed between experimental loading contents for (a) COU, (b) CUR), (c) NIL and α-adjusted Flory–Huggins interaction parameters ($\chi_{ca,ANG}$). Thus, a clear influence of the hydrophobic structure on the LC is visible. LC values were obtained from the co-solvent method and $\chi_{ca,ANG}$ was calculated by individual solubility parameters from the YMB method.

2586 | J. Mater. Chem. B, 2026, **14**, 2578–2593

This journal is © The Royal Society of Chemistry 2026

Fig. 7 Combination of COU, CUR, and NIL with ANGs containing different amounts (10–40 mol%) of HEXA and CHOLA – strong negative linear correlations are observed between experimental loading contents for (a) COU, (b) CUR), (c) NIL and α-adjusted Flory–Huggins interaction parameters ($\chi_{ca,ANG}$). Thus, for a specific hydrophobic structure, a clear influence of the hydrophobic content is visible. LC values were obtained from the co-solvent method and $\chi_{ca,ANG}$ was calculated by individual solubility parameters from the YMB method.
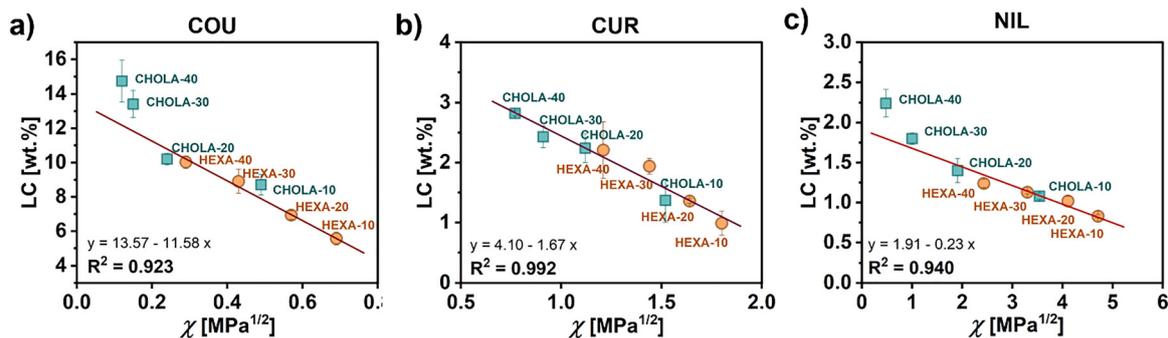
Overall, these results suggest that cargo–ANG miscibility can be used as a key determinant in estimating loading contents: for a given cargo, LC can also be maximized by adjusting the ANGs' hydrophobic content since $\chi_{ca,ANG}$ mainly depends on network composition. Interestingly, similar LCs can be achieved with different ANG compositions. For example, CHOLA-20 and HEXA-40 perform similarly for the loading of COU, CUR, and NIL. This indicates that comparable $\chi_{ca,ANG}$ values can result from either a higher content of less hydrophobic HEXA groups or a lower content of more hydrophobic CHOLA groups. Such structural versatility is particularly valuable when considering additional interactions of the ANG network with biological systems. For instance, we recently showed that protein adsorption is strongly influenced by the type of hydrophobic group in the ANG.[19] In this context, our findings could help to identify the optimum ANG composition that maximizes LC and minimizes protein adsorption.

Part D: integrating all correlations into a master curve as quantitative model for cargo loading in amphiphilic nanogels.

We observed strong correlations between LC and $\chi_{ca,ANG}$ across a wide range of cargo–ANG combinations. Specifically, we showed that a cargo's LC linearly depends on both the structure (part B – Fig. 6) and molar content (part C – Fig. 7) of hydrophobic groups in the ANG network. Notably, the fits in both cases show similar slopes and y-intercepts for each model cargo, e.g., similar fits for COU in Fig. 5a and 6a, for CUR in Fig. 5b and 6b, and for NIL in Fig. 5c and 6c. This consistency suggests a general relationship between LC and ANG network composition.

To test this hypothesis, we combined the datasets of part B and part C in a single plot. Fig. 8a shows the LCs of COU, CUR, and NIL in all ANGs. For each cargo, LC again correlates linearly with $\chi_{ca,ANG}$ but shows a different slope. We observed slopes and corrected R^2 values for COU of -13.74 and 0.928, for CUR of -1.73 and 0.978, and for NIL of -0.23 and 0.949. These trends confirm that, for a given cargo, LC generally depends on ANG network composition as determined by both the structure (BENZA-20, HEXA-20, DODA-20, BDODA-20, and CHOLA-20)
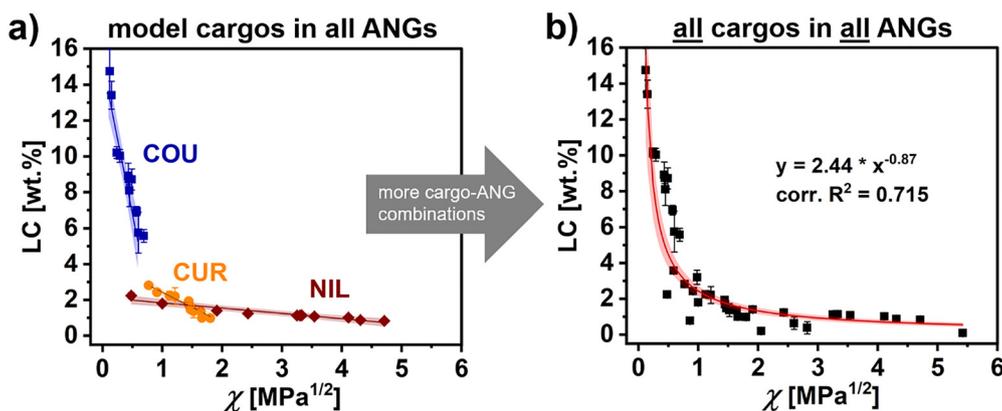

Fig. 8 Combination of all cargos with all ANG compositions – a universal correlation between LC and ANG composition is suggested as follows: (a) combining the influence of ANGs hydrophobic structure (part B) and molar content (part C) results in individual linear correlations between LC and $\chi_{ca,ANG}$ for COU, CUR, and NIL. The overlap between the linear fits suggests that these may represent tangents to a single, unified trend curve. (b) Addition of data for other cargos (part A) to the combined data for COU, CUR, and NIL results in a strong monotonically decreasing correlation between LC and $\chi_{ca,ANG}$. This correlation can be described best by an allometric power curve which could serve as master curve to guide ANG design towards maximized drug loading. Areas around the fit curves represent 95% confidence intervals of the respective fits.

This journal is © The Royal Society of Chemistry 2026

J. Mater. Chem. B, 2026, **14**, 2578–2593 | **2587**

and the molar content (HEXA-10–HEXA-40 and CHOLA-10–CHOLA-40) of hydrophobic groups. While the linear fits show different slopes for each cargo, their overlap suggests they may represent tangents to a single, unified trend curve.

Evaluating this assumption, we included the additional cargo data from part A into the plot. As shown in Fig. 8b, LC exhibits a strong monotonic negative correlation with $\chi_{ca,ANG}$ across all combinations of cargo and ANG composition. This trend is best described by an allometric power fit (corr. $R^2 = 0.715$; see SI, Fig. S28 for comparison with exponential fit). Generally, allometric models effectively capture non-linear scaling as often observed in complex systems.[46,47] They are commonly used in biology and materials science to describe how different properties scale with each other across varying samples.[48–50] In our case, the relationship between LC and α-adjusted $\chi_{ca,ANG}$ likely reflects underlying structural and compositional factors in the ANG network that do not scale linearly. Thus, the allometric fit accommodates this behaviour, allowing us to capture the general trend across different cargo–ANG combinations with a single, correlation-based model. This is in direct contrast to standard Hansen solubility models that are based on R_a (see SI, Fig. S29 for comparison). As a result, we suggest that the fitted trend could serve as a master curve to roughly guide ANG design towards maximized drug loading.

3. Conclusions

In this work, a numerical framework was established to correlate molecular and material parameters with the drug loading content (LC) of amphiphilic nanogels (ANGs). By applying Flory–Huggins theory and systematically adjusting the correction factor α, the interaction between hydrophobic cargos and ANG networks was described. The results demonstrate that the Flory–Huggins interaction parameter χ, when combined with an appropriate α value, correlates strongly with experimentally determined LC for a broad range of cargos and ANG compositions.

The use of differentiated α values for dispersion-dominated, polar, and hydrogen-bond – dominated cargos significantly improves the applicability of χ as a numerical measure for ANG–cargo compatibility compared to approaches using a uniform correction factor α. The obtained correlations enable a rational comparison of different hydrophobic side groups and their content within the ANG network. They also provide guidance for the selection of ANG compositions with improved loading performance.

In this study, poly(methacrylamide)-based amphiphilic nanogels were deliberately chosen as a well-defined and extensively characterized model system. For this system, detailed insight into cargo loading mechanisms and network–cargo interactions is already available from previous work. This allows the present study to focus on the development and validation of the α-adjusted Flory–Huggins framework rather than on the specific chemistry of the carrier platform. Since the underlying concept relies on general solubility parameters

and polymer–solute interaction theory, the approach is not intrinsically limited to poly(methacrylamide) networks. In principle, it is transferable to other amphiphilic polymer networks, provided that appropriate parametrization and experimental validation are performed.

It should be noted that the present framework is empirically calibrated using experimentally determined LC and therefore does not yet constitute a fully predictive model. The calculated χ values represent effective interaction parameters that account for non-idealities such as heterogeneous network structures and multiple interaction contributions. Consequently, true prediction of drug loading content would require blind validation, in which LC is estimated prior to experimental determination. With respect to application, the present framework addresses the formulation stage by guiding the selection and optimization of ANG compositions for loading poorly water-soluble drugs. It does not aim to predict biological performance or clinical outcome. Accordingly, the present study is limited to physicochemical aspects of cargo loading *in vitro*, and further biological and *in vivo* evaluation could be performed in future studies to establish similar quantitative models regarding other properties that influence the performance of drug delivery systems. For instance, it is expected that drug–polymer interactions have an impact on drug stability in circulation, protein corona formation, release kinetics, or biodistribution.

Although the present study is based on a limited but chemically diverse dataset, the established correlation framework could, in principle, be extended in the future to larger data collections. In such a context, data-driven analysis could be used to systematically compare the performance of the present χ-based descriptors with alternative physicochemical descriptors (*e.g.*, cLogP, Hansen distance, or related solubility-based metrics) and to examine non-linear correlations between interaction parameters and experimentally determined loading contents. Moreover, combining the present dataset with published datasets from other polymer–drug formulation studies (*e.g.*, Luxenhofer and co-workers)[29] could allow a more rigorous assessment of the robustness and transferability of the approach to chemically distinct polymer carrier systems. In this sense, data-driven methods would not replace the present physically motivated framework, but could support its extension and validation once sufficiently broad and consistent datasets become available.

4. Experimental section

4.1. Materials

All substances and reagents were purchased from commercially available sources and were used as received, unless otherwise described.[20,22] Pentafluorophenyl methacrylate (PFPMA)[51,52] and amine-functionalized cholesterol (CHOLA)[53,54] were synthesized as described previously. Poly(pentafluorophenyl methacrylate) (PPFPMA) reactive precursor particles were synthesized following a modified literature procedure.[40] Functionalization of PPFPMA precursor particles was performed as

2588 | *J. Mater. Chem. B*, 2026, **14**, 2578–2593

This journal is © The Royal Society of Chemistry 2026

described in our previous work.[20] Triethylamine (TEA, 99% purity) and benzylamine (BENZA, 98% purity) were purchased from ABCR. Hexylamine (HEXA, 99% purity), 2-butyl-n-octan-1-amine (BDODA, 98% purity) and ammonium persulfate (APS, 99% purity) were obtained from TCI. Dodecylamine (DODA, 98% purity) was purchased from Alfa Aesar. Ethylene glycol dimethacrylate (EGDMA, 98% purity), amino-2-propanol (HPA, 93% purity), and dodecyl sulfate sodium salt (SDS, 95% purity) were purchased from Merck, Germany. Curcumin (from Turmeric rhizome; total curcuminoid content ≥95%) was provided by ABCR, Germany. Berberine chloride (purity ≥98%), dexamethasone (purity ≥98%), Sudan I (dye content ≥95%), coumarin (purity ≥99%) and loteprednol etabonate (purity ≥98%) were purchased from Sigma-Aldrich, USA. Nile Red (purity ≥98%) was from Fluorochem, UK. Paclitaxel (purity ≥98%), meloxicam (purity ≥98%), efavirenz (purity ≥98%) and telmisartan (purity ≥98%) were from TCI, India. All drugs and dyes were used as received without further purification. Dialysis was performed in regenerated cellulose dialysis tubes from Repligen, USA (Spectra/Por® 4 width: 45 mm, MWCO 12 000–14 000 g mol^{-1}).

4.2. Methods

ATR-FTIR. FT-IR spectra by attenuated total reflection (ATR) were recorded on a PerkinElmer two spectrometer measuring between 4000 and 650 cm^{-1} (PerkinElmer, Waltham, USA). All data was obtained from the software Spectrum (version 10.4.4) by PerkinElmer.

Dynamic light scattering (DLS). Particle size distributions and hydrodynamic diameters were determined by dynamic light scattering using Nicomp Nano Z3000 (Particle Sizing Systems, USA). For measurements, the respective ANGs were freeze dried and redispersed in water by stirring and sonication. Measurements of the diluted dispersions in water were conducted at room temperature and 90° scattering angle. Reported hydrodynamic diameters represent the intensity-weighted diameters obtained from the NICOMP algorithm Nano Z3000 (Particle Sizing Systems).

UV/Vis. UV/Vis was performed on a Tecan Infinite M100 PRO plate reader (Tecan Trading AG, Männedorf, Switzerland). Measurements were done in a 96 flat bottom clear cyclic olefin copolymer well plate (UV-star®, Greiner Bio-One International GmbH, Kremsmünster, Austria). All data were processed using the software SparkControl (see SI, Fig. S7–S12 for calibration curves).

HPLC. A reverse phase Supelco C18 column (Supelco, Nucleosil 100 C18, 25 × 4.6 cm, 5 μm) was used for all the HPLC methods (Agilent Technologies, Santa Clara, CA, USA). All methods were previously described in the literature and were used with minor modifications (see SI, Fig. S13–S17 for calibration curves).[55–59]

Transmission electron microscopy (TEM). Samples were prepared by placing a 10 μL droplet of nanogel solution (1 mg mL^{-1} in ultrapure water) onto a carbon-coated copper grid (400 mesh, Quantifoil Micro Tools GmbH, Großlöbichau, Germany) and allowing it to interact for 45 s. The excess liquid

was gently removed by blotting with filter paper. This procedure was repeated ten times. The prepared grids were then left to air-dry overnight. For contrast enhancement, the TEM samples were exposed to iodine vapor in a sealed chamber for 15 minutes prior to imaging. Afterwards, particles were measured using the TEM mode of a Hitachi SU8030 scanning electron microscope (Hitachi High-Technologies Corporation, Tokyo, Japan) used at a working voltage of 30.0 kV, with imaging at various magnifications.

4.3. Nanogel library: synthesis and characterization

Synthesis of reactive poly(pentafluorophenyl methacrylate) PPFPMA precursor particles. Reactive precursor particles were synthesized *via* free-radical emulsion polymerization as recently described.[22,40] In brief, the dispersed phase was prepared from a mixture of 20.00 g of PFPMA (79.2 mmol, 1.0 eq.) and 0.316 g of EGDMA (1.58 mmol, 0.02 eq.) (filtered over aluminium oxide). The aqueous phase consisted of 360 mL of an aqueous SDS solution (1.25 mg mL^{-1}). Both phases were combined and sonicated for 10 min. The resulting emulsion was purged with nitrogen for 10 min and heated up to 60 °C in an oil bath. After 30 min, 20 mL of previously degassed aqueous APS solution (10 mg mL^{-1}) were added to the reaction mixture. The reaction was stirred with 700 rpm at 60 °C for 72 h.

Afterwards, the resulting precursor particles were purified by centrifugation (30 min, 10 000 rpm) and redispersion in DI water (5 cycles). Redispersion was achieved by using a vortex and an ultrasonication bath between each centrifugation step. Purified particles in water were analyzed *via* TEM (see SI, Fig. S4) and dynamic light scattering (DLS) to determine particle size and particle size distribution (see SI, Fig. S5 and S6). Afterwards, the particles were freeze-dried, yielding a white powder with an average yield of 70%. Dried particles were investigated by ATR-FTIR spectroscopy regarding potential hydrolysis of reactive ester groups (see SI, Fig. S2 and S3).

Post-polymerization functionalization of reactive PPFPMA precursor particles. Functionalization of precursor particles was performed following our previously reported procedure.[20] In a round bottom flask, freeze-dried PPFPMA particles (400 mg, 1.59 mmol w.r.t. monomer units of PPFPMA particles, 1.0 eq.) were resuspended in 80 mL DMF by sonication in an ultrasonication bath. Precursor particles were left to swell overnight before a mixture of a hydrophobic moiety (BENZA, HEXA, DODA, BDODA or CHOLA) and the hydrophilic amine (HPA) was added. While the molar ratio between hydrophobic and hydrophilic amine was varied, the total amount of both moieties together was always 3.0 eq. w.r.t. PFPMA units. Additionally, 3 eq. of TEA were added and the reaction was stirred at 50 °C for 3 days. Upon completion of the reaction, the particles were dialyzed extensively for more than 10 days in total. First, against DMF, second against DI water, and third, against Milli-Q water. Afterwards the particles were centrifuged (10 000 rpm, 1 h) and redispersed in a reduced volume of Milli-Q water to increase the particle concentration. The redispersed suspensions were examined *via* TEM (SI, Fig. S4) and investigated by DLS to

determine the hydrodynamic diameter (see SI, Fig. S5 and S6). Afterwards, ATR-FTIR spectroscopy of freeze-dried aliquots was used to monitor the conversion of the post-polymerization modification (see SI, Fig. S2 and S3).

4.4. Loading of nanogel library with drugs and dyes

Loading by the co-solvent method. Loading of compounds from the library followed our previously described procedure.[20] Here, 2.5 mL of each drug/dye solution in acetone at 0.2 mg mL^{-1} were added to 5 mL of an aqueous ANG suspension at 1 mg mL^{-1} (final feed ratio of drug/dye w.r.t. the ANGs: 10 wt%). The mixtures were stirred open to air for 48 h to evaporate the organic solvent. Afterwards, the volume of evaporated water was determined by the difference of weight with respect to the initial 5 mL and replaced. Suspensions of loaded ANGs were filtered through cotton and syringe filters (0.8 μm, cellulose mixed ester) to remove any non-incorporated precipitates of the compounds. All samples were prepared in triplicate.

Loading by the film uptake method. A solution of drug or dye in acetone (2.5 mL, 0.2 mg mL^{-1}) was placed into a glass vial (10 mL). The organic solvent was evaporated thus giving a thin film of drug or dye on the bottom of the vial. Afterwards, 5 mL of an aqueous ANG suspension (1 mg mL^{-1}) were added and stirred at room temperature overnight. Finally, the samples were processed as in the co-solvent method described above. All samples were prepared in triplicate.

Drug/dye content determination. Aqueous suspensions of loaded ANGs were freeze-dried and re-suspended in a defined amount of solvent that is suitable for cargo dissolution and ANG swelling. The amount of incorporated cargo was determined *via* UV/Vis spectroscopy or reverse phase-HPLC (see methods and gradients in the SI, Fig. S7–S17). Each sample was prepared and analyzed in triplicate. The cargo loading was reported as loading content (LC) based on eqn (2):

$$LC = \frac{m_{cargo}}{m_{ANG}} \times 100\% \tag{2}$$

where m_{cargo} is the mass of cargo measured in the resuspended ANGs, and m_{ANG} is the mass of the freeze-dried ANGs of each aliquot. Cargo quantities were corrected by subtracting the residual amount of drug/dye dissolved in water instead of encapsulated in the ANGs. For this, control experiments were performed that mimic the respective loading method (co-solvent/film uptake) but use pure water instead of ANG suspensions.

4.5. Determination of solubility parameters and calculation of Flory–Huggins interaction parameters

The Flory–Huggins interaction parameters (χ) between the amphiphilic nanogels' polymer network and the different cargos were calculated from the individual Hansen solubility parameters for ANG ($\delta_{D,ANG}$, $\delta_{P,ANG}$, $\delta_{H,ANG}$) and cargo (ca) ($\delta_{D,ca}$, $\delta_{P,ca}$, $\delta_{H,ca}$):[25,35]

$$\chi_{ca,ANG} = \alpha \frac{V_{m,ca}}{RT}\Big[\big(\delta_{D,ca} - \delta_{D,ANG}\big)^2 + 0.25\big(\delta_{P,ca} - \delta_{P,ANG}\big)^2$$
$$+ 0.25\big(\delta_{H,ca} - \delta_{H,ANG}\big)^2\Big] \tag{3}$$

Here, δ_D represents the contribution of dispersion forces, δ_P the contribution of polar interactions, and δ_H the influence of hydrogen bonds. In each parameter, ca stands for the cargo (drug or dye), and ANG stands for the network polymer. α is the correction factor, $V_{m,ca}$ is the molar volume of the cargo, R is the gas constant 8.314 J (mol K)$^{-1}$, and T is the temperature (in our case $T = 293.15$ K).

The molar volume of the cargo was calculated *via* the indirect group contribution method (GCM) by Fedor.[27,42] Here, the molar volume (V_m) is defined as the sum of individual volumes and numbers for different structural groups i that make up a compound:

$$V_m = \sum n_i V_i \tag{4}$$

Values for the volumes of individual groups can be found in the literature and their contributions are listed in the SI, Tables S8–S18.[27] Calculated values for $V_{m,ca}$ are listed in the SI, Table S21.

Hansen solubility parameters for cargos and ANGs were calculated from two different methods: The method from Hoftyzer and van Krevelen (HVK)[27] or the Yamamoto molecular break (YMB)[29] method.

Calculation of HSP *via* HVK. In the HVK method, the individual solubility parameters for the dispersion forces, polar interactions and hydrogen bonds are calculated from the sum of contributions from different structural groups for the respective molecule according to:[25,27]

$$\delta_D = \frac{\sum F_{di}}{V_m} \tag{5}$$

$$\delta_P = \frac{\sqrt{\sum F_{pi}^2}}{V_m} \tag{6}$$

$$\delta_H = \sqrt{\frac{\sum E_{hi}}{V_m}} \tag{7}$$

Here, i denotes the index of the structural groups, F_d is the dispersion component of the molar attraction function, F_p is the polar component of the molar attraction function, and E_h is the contribution of hydrogen bonding forces to the cohesive energy. The values of F_{di}, F_{pi}^2, E_{hi} for each structural group i can be found in the literature.[25,27] Their sums are denoted as $F_D = \sum F_{di}$, $F_P^2 = \sum F_{pi}^2$, and $E_H = \sum E_{hi}$. For all, V_m is the molar volume.

For the cargos, V_m was calculated by Fedors' method as stated above.[42] The values of molar attractive forces (F_{di}, F_{pi}) and energy of hydrogen bonding (F_{hi}) were taken from the literature for each assigned functional group

2590 | *J. Mater. Chem. B*, 2026, **14**, 2578–2593

This journal is © The Royal Society of Chemistry 2026

(see SI, Tables S8–S18).[27] Combination with the V_m values gave the solubility parameters (see SI, Table S19).

For the ANGs, the calculation needs to consider the random copolymer structure of the network. Here, the copolymer chains contain a mixture of two different monomers, *e.g.*, poly(2-hydroxypropylmethacrylamide-*co*-hexylmethacrylamide) P(HPMA-*co*-HEXMA). Thus, the molar volume and the different energy contributions need to be calculated for each type of repeating unit, *i.e.*, $V_{m,HPMA}$; $V_{m,HEXMA}$, $F_{D,HPMA}$, $F_{D,HEXMA}$, $F_{P,HPMA}^2$, $F_{P,HEXMA}^2$, $E_{H,HPMA}$, and $E_{H,HEXMA}$. This can be done from literature values for the different structural groups in the respective group contribution method, *i.e.*, Fedors' method for V_m and HVK for the energy contributions. Furthermore, the molar fractions of the different monomers need to be considered. Thus, for P(HPMA-*co*-HEXMA), the molar fraction of HPMA in the copolymer is represented by f_{HPMA} and the molar fraction of HEXMA is represented by f_{HEXMA}. Similarly, the molar volume of HPMA is denoted as $V_{m,HPMA}$, while the molar volume of HEXMA is denoted as $V_{m,HEXMA}$, respectively. The overall number of repeating units in each chain does not influence the Hansen solubility parameters and can be neglected. Taking these considerations into account, the three components of the Hansen solubility parameters for the network copolymers can be calculated by:

$$\delta_D = \frac{f_{HPA}F_{D,HPA} + f_{HEXMA}F_{D,HEXMA}}{f_{HPA}V_{m,HPA} + f_{HEXMA}V_{m,HEXMA}} \tag{8}$$

$$\delta_P = \frac{\sqrt{f_{HPA}^2 F_{P,HPA}^2 + f_{HEXMA}^2 F_{P,HEXMA}^2}}{f_{HPA}V_{m,HPA} + f_{HEXMA}V_{m,HEXMA}} \tag{9}$$

$$\delta_H = \sqrt{\frac{f_{HPA}E_{H,HPA} + f_{HEXMA}E_{H,HEXMA}}{f_{HPA}V_{m,HPA} + f_{HEXMA}V_{m,HEXMA}}} \tag{10}$$

The values of F_D, F_P^2, E_H and V_m for one repeating unit of the different hydrophobic co-units were taken from the literature for each assigned functional group. Group assignments are summarized in the SI, Tables S1–S7.[27] The resulting solubility parameters δ_D, δ_P, and δ_H are listed in the SI in Table S7 for the nanogels and in the SI in Table S19 for all the cargos. Furthermore, the derived Flory–Huggins interaction parameters for combinations of CHOLA-20 ANGs and all cargos are listed in the SI in Table S22 for Lindvig's method (α = 0.6), Hansen framework (α = 1) and α-adjusted calculations.

Calculation of HSP *via* YMB. In the YMB method, the individual solubility parameters are also calculated from the sum of contributions from different structural groups. However, the calculations are performed by a semi-empirical group contribution and optimization algorithm in the commercially available software Hansen solubility parameters in practice (HSPiP). As input, the respective SMILES codes (obtained from ChemDraw Professional 15.2.) were used for each compound of interest. While the calculations for the small molecule drugs and dyes are straightforward, the calculations for the ANG networks need to consider the copolymer structure again. For this, it is suggested to treat the random copolymer networks

as a mixture of two homopolymers.[60] In the software, this can be performed through the "polymer blends" option: in brief, the amphiphilic copolymers are divided into their respective hydrophilic and hydrophobic repeat units. These repeat units are then considered as homopolymers for which a respective SMILES code can be entered. The hydrophobic content of each copolymer network is then represented as the relative mass fraction of the hydrophobic homopolymer in the blend. For example, a CHOLA-20 network, that consists of P(HPMA₈₀-*co*-CHOLMA₂₀), is considered as a mixture of 80% PHPMA and 20% PCHOLMA. In all cases a weighted approach was used to calculate V_m of the cargo *via* Fedors' method as described above (see SI, Table S21 for calculated values).

The resulting weighted solubility parameters δ_D, δ_P, and δ_H for all the ANGs are listed in the SI in Table S7. The values for all cargos are listed in Table S19. Derived Flory–Huggins interaction parameters for combinations of CHOLA-20 ANGs and all cargos are listed in the SI in Table S22 for Lindvig's method (α = 0.6), Hansen framework (α = 1) and α-adjusted calculations.

Calculation of Hildebrand solubility parameters. Hildebrand solubility parameters were calculated as described in the SI (Section 2.3). Calculated values for molar volume and cohesive energies are listed for ANGs and cargos in Tables S20 and S21, respectively. Resulting Hildebrand solubility parameters are listed in SI Table S23.

Calculation of the distance R_a between total Hansen solubility parameters of ANG and cargo. The distances between d_T of ANG and cargo were calculated by the HVK and YMB method as described in the SI. Resulting values are shown in SI in Tables S24–S30.

Conflicts of interest

There are no conflicts to declare.

Data availability

Supplementary information is available. See DOI: https://doi.org/10.1039/d5tb02138c.

The data supporting this article have been included as part of the supplementary information (SI) and raw data are available *via* Zenodo, DOI: https://doi.org/10.5281/zenodo.17174901.

Acknowledgements

This journal is © The Royal Society of Chemistry 2026

J. Mater. Chem. B, 2026, **14**, 2578–2593 | **2591**

References

1 S. M. Paul, D. S. Mytelka, C. T. Dunwiddie, C. C. Persinger, B. H. Munos, S. R. Lindborg and A. L. Schacht, *Nat. Rev. Drug Discovery*, 2010, **9**, 203–214.

2 J. A. DiMasi, R. W. Hansen and H. G. Grabowski, *J. Health Econ.*, 2003, **22**, 151–185.

3 R. Ghadi and N. Dand, *J. Controlled Release*, 2017, **248**, 71–95.

4 C.-M. Lehr and J. Haas, *Expert Opin. Biol. Ther.*, 2002, **2**, 287–298.

5 A. Rösler, G. W. M. Vandermeulen and H.-A. Klok, *Adv. Drug Delivery Rev.*, 2001, **53**, 95–108.

6 D. Peer, J. M. Karp, S. Hong, O. C. Farokhzad, R. Margalit and R. Langer, *Nat. Nanotechnol.*, 2007, **2**, 751–760.

7 S. Mura, J. Nicolas and P. Couvreur, *Nat. Mater.*, 2013, **12**, 991–1003.

8 J. K. Oh, R. Drumright, D. J. Siegwart and K. Matyjaszewski, *Prog. Polym. Sci.*, 2008, **33**, 448–477.

9 D. Gan and L. A. Lyon, in *Smart Colloidal Materials*, ed. W. Richtering, Springer, Berlin, Heidelberg, 2006, vol. 133, pp. 1–8.

10 ed. A. Pich and W. Richtering, *Chemical Design of Responsive Microgels*, Springer, Berlin, Heidelberg, 2011, vol. 234.

11 D. Klinger and K. Landfester, *Polymer*, 2012, **53**, 5209–5231.

12 C. López-Iglesias and D. Klinger, *Macromol. Biosci.*, 2023, **23**, 2300256.

13 X. Zhang, S. Malhotra, M. Molina and R. Haag, *Chem. Soc. Rev.*, 2015, **44**, 1948–1973.

14 S. Nayak and L. A. Lyon, *Angew. Chem., Int. Ed.*, 2005, **44**, 7686–7708.

15 C. Biglione, T. M. P. Neumann-Tran, S. Kanwal and D. Klinger, *J. Polym. Sci.*, 2021, **59**, 2665–2703.

16 A. F. Thünemann, A. Gruber and D. Klinger, *Langmuir*, 2020, **36**, 10979–10988.

17 Z. Jiang, H. Liu, H. He, A. E. Ribbe and S. Thayumanavan, *Macromolecules*, 2020, **53**, 2713–2723.

18 L. Jiang, Z. Luo, X. J. Loh, Y.-L. Wu and Z. Li, *ACS Appl. Bio Mater.*, 2019, **2**, 3591–3600.

19 T. Bewersdorff, A. Gruber, M. Eravci, M. Dumbani, D. Klinger and A. Haase, *Int. J. Nanomed.*, 2019, **14**, 7861–7878.

20 A. Gruber, D. Işık, B. B. Fontanezi, C. Böttcher, M. Schäfer-Korting and D. Klinger, *Polym. Chem.*, 2018, **9**, 5572–5584.

21 K. Letchford, R. Liggins and H. Burt, *J. Pharm. Sci.*, 2008, **97**, 1179–1190.

22 C. López-Iglesias, A. Markovina, N. Nirmalananthan-Budau, U. Resch-Genger and D. Klinger, *Nanoscale*, 2024, **16**, 9525–9535.

23 K. Kothari, V. Ragoonanan and R. Suryanarayanan, *Mol. Pharmaceutics*, 2015, **12**, 162–170.

24 L. M. Johnson, Z. Li, A. J. LaBelle, F. S. Bates, T. P. Lodge and M. A. Hillmyer, *Macromolecules*, 2017, **50**, 1102–1112.

25 C. M. Hansen, *Hansen Solubility Parameters: A User's Handbook*, CRC Press, 2nd edn, 2007.

26 J. U. Wieneke, B. Kommoß, O. Gaer, I. Prykhodko and M. Ulbricht, *Ind. Eng. Chem. Res.*, 2012, **51**, 327–334.

27 D. W. Van Krevelen and K. Te Nijenhuis, *Properties of Polymers*, Elsevier, 1997, pp. 189–227.

28 E. R. Turpin, V. Taresco, W. A. Al-Hachami, J. Booth, K. Treacher, S. Tomasi, C. Alexander, J. Burley, C. A. Laughton and M. C. Garnett, *Mol. Pharmaceutics*, 2018, **15**, 4654–4667.

29 M. M. Lübtow, M. S. Haider, M. Kirsch, S. Klisch and R. Luxenhofer, *Biomacromolecules*, 2019, **20**, 3041–3056.

30 Y. Tian, C. Shi, Y. Sun, C. Zhu, C. C. Sun and S. Mao, *Mol. Pharmaceutics*, 2015, **12**, 816–825.

31 C. Shi, Y. Sun, H. Wu, C. Zhu, G. Wei, J. Li, T. Chan, D. Ouyang and S. Mao, *Int. J. Pharm.*, 2016, **512**, 282–291.

32 J.-P. Latere Dwan'Isa, L. Rouxhet and V. Préat, *et al.*, *Pharmazie*, 2007, 499–504.

33 A. O. Kasimova, G. M. Pavan, A. Danani, K. Mondon, A. Cristiani, L. Scapozza, R. Gurny and M. Möller, *J. Phys. Chem. B*, 2012, **116**, 4338–4345.

34 A. Erlebach, T. Ott, C. Otzen, S. Schubert, J. Czaplewska, U. S. Schubert and M. Sierka, *J. Comput. Chem.*, 2016, **37**, 2220–2227.

35 T. Lindvig, M. L. Michelsen and G. M. Kontogeorgis, *Fluid Phase Equilib.*, 2002, **203**, 247–260.

36 M. J. Louwerse, A. Maldonado, S. Rousseau, C. Moreau-Masselon, B. Roux and G. Rothenberg, *ChemPhysChem*, 2017, **18**, 2999–3006.

37 P. Ruelle, M. Buchmann, H. Nam-Tran and U. W. Kesselring, *Pharm. Res.*, 1992, **9**, 788–791.

38 P. Ruelle, C. Rey-Mermet, M. Buchmann, H. Nam-Tran, U. W. Kesselring and P. L. Huyskens, *Pharm. Res.*, 1991, **8**, 840–850.

39 T. Lindvig, M. L. Michelsen and G. M. Kontogeorgis, *AIChE J.*, 2001, **47**, 2573–2584.

40 R. Cui, M. Ickler, A. Markovina, S. Kanwal, N. Vogel and D. Klinger, *ACS Nano*, 2024, **18**, 25499–25511.

41 A. Gruber, L. Navarro and D. Klinger, *Adv. Mater. Interfaces*, 2020, **7**, 1901676.

42 R. F. Fedors, *Polym. Eng. Sci.*, 1974, **14**, 147–154.

43 M. Romay, N. Diban and A. Urtiaga, *Polymers*, 2021, **13**, 678.

44 C. Barth and B. A. Wolf, *Macromol. Chem. Phys.*, 2000, **201**, 365–374.

45 F. Leroy, *Soft Mater.*, 2013, **11**, 231.

46 G. B. West, J. H. Brown and B. J. Enquist, *Science*, 1997, **276**, 122–126.

47 J. R. Banavar, A. Maritan and A. Rinaldo, *Nature*, 1999, **399**, 130–132.

48 A. M. Makarieva, V. G. Gorshkov, B.-L. Li, S. L. Chown, P. B. Reich and V. M. Gavrilov, *Proc. Natl. Acad. Sci. U. S. A.*, 2008, **105**, 16994–16999.

49 J. D. Damuth, *Nature*, 1998, **395**, 115–116.

50 L. J. Gibson, M. F. Ashby and B. A. C. Harley, *Cellular materials in nature and medicine*, Cambridge Univ. Press, Cambridge, 2010.

51 J.-C. Blazejewski, J. W. Hofstraat, C. Lequesne, C. Wakselman and U. E. Wiersum, *J. Fluorine Chem.*, 1998, **91**, 175–177.

52 M. Eberhardt, R. Mruk, R. Zentel and P. Théato, *Eur. Polym. J.*, 2005, **41**, 1569–1575.

2592 | *J. Mater. Chem. B*, 2026, **14**, 2578–2593

This journal is © The Royal Society of Chemistry 2026

53 M. D. Kearns, A.-M. Donkor and M. Savva, *Mol. Pharmaceutics*, 2008, **5**, 128–139.

54 Y. Nie, M. Günther, Z. Gu and E. Wagner, *Biomaterials*, 2011, **32**, 858–869.

55 X. Farto-Vaamonde, G. Auriemma, R. P. Aquino, A. Concheiro and C. Alvarez-Lorenzo, *Eur. J. Pharm. Biopharm.*, 2019, **141**, 100–110.

56 HPLC Determination of Meloxicam on Newcrom R1 Column, https://sielc.com/hplc-determination-of-meloxicam.

57 Y. K. Han and A. I. Segall, *J. Chromatogr. Sci.*, 2015, **53**, 761–766.

58 M. V. Barbosa, L. O. F. Monteiro, A. R. Malagutti, M. C. Oliveira, A. D. Carvalho-Junior and E. A. Leite, *J. Braz. Chem. Soc.*, 2015, **26**, 1338–1343.

59 S. Wankhede, M. Tajne, K. Gupta and S. Wadodkar, *Indian J. Pharm. Sci.*, 2007, **69**, 298.

60 S. Abbott, C. M. Hansen and H. Yamamoto, Hansen solubility parameters (HSPiP) [Software and eBook], HansenSolubility.com, 2008.

This journal is © The Royal Society of Chemistry 2026

J. Mater. Chem. B, 2026, **14**, 2578–2593 | **2593**